

Supporting Information

Efficient and Robust Heteronuclear Cross-Polarization for High-Speed-Spinning Biological Solid-State NMR Spectroscopy

Sheetal Jain, Morten Bjerring, and Niels Chr. Nielsen*

Center for Insoluble Protein Structures (inSPIN), Interdisciplinary Nanoscience Center (iNANO) and Department of Chemistry, Aarhus University, DK-8000 Aarhus C, Denmark.

*Corresponding author: ncn@inano.au.dk

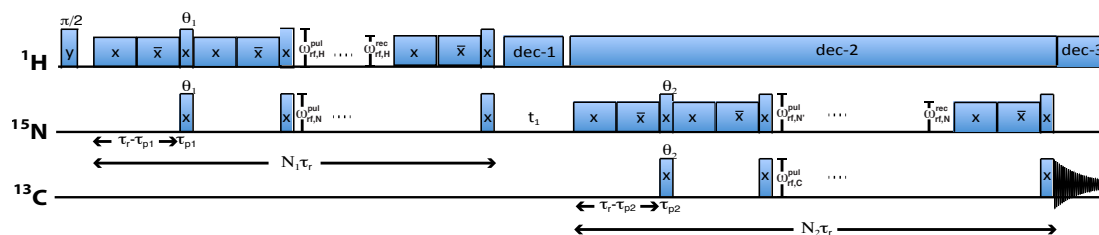


Figure S1. Detailed 2D pulse sequence for NCA/NCO experiments outlining typical $^1\text{H} \rightarrow ^{15}\text{N}$ (before the t_1 period) and $^{15}\text{N} \rightarrow ^{13}\text{C}$ (after the t_1 period) elements using $^{\text{RESPIRATION}}\text{CP}$. The initial $(\pi/2)_y$ pulse generates x -phase coherence on the ^1H spins, which in the first element is transformed to x -phase coherence on the ^{15}N spins, which subsequently is transferred to x -phase coherence on the ^{13}C spins. Each $^{\text{RESPIRATION}}\text{CP}$ element contains the element in Fig. 1a repeated N_1 and N_2 rotor periods for the $^1\text{H} \rightarrow ^{15}\text{N}$ and $^{15}\text{N} \rightarrow ^{13}\text{C}$ coherence transfers, respectively, with each rotor period contain one small-flip-angle pulse on each channel (upon irradiation in several rotor periods these takes the form of a $^{\text{RESPIRATION}}\text{pulse}^1$ on each channel interleaved with phase-alternated CW irradiation on one of the rf channels for dipolar recoupling). For each rotor period the length of the CW irradiation (half of it with phase x , half of it with phase $-x$) correspond to a rotor period minus the length of the small flip-angle pulse (θ).

1. Experiments

All experiments were performed on a Bruker Avance 400 (9.4 T, 400 MHz for ^1H) wide-bore NMR spectrometer equipped with a standard triple-resonance 2.5 mm MAS probe. The spectra were acquired using 30 kHz sample spinning, 3 s repetition delay, 122 kHz decoupling during $^{15}\text{N} \rightarrow ^{13}\text{C}$ coherence transfer (marked “dec-2” in Fig. S1; although the experiments also works without decoupling, this provided the most representative case relative to standard experiments in the field), and 139 kHz decoupling during acquisition (marked “dec-3 in Fig. S1). The experiments in Figs. 1d and 1e used 1024 scans, with the standard CP spectrum (red) in Fig. 1d recorded using ^1H - ^{15}N cross-polarization with rf field strengths of 70 (average) and 40 kHz on ^1H and ^{15}N , respectively, with a 80-100% ramp² at the ^1H channel during the 350 μs contact time. The $^{\text{RESPIRATION}}\text{CP}$ spectrum (red) in Fig. 1d was recorded using 60 kHz rf field strength on the ^1H channel for recoupling ($\omega_{\text{rf},\text{H}}^{\text{rec}} / (2\pi)$ in the notation of Fig. S1), and also with 60 kHz rf field strength for each of the 3.5 μs ($\theta \approx 75^\circ$) $^{\text{RESPIRATION}}$

pulses¹ on both the ¹H and ¹⁵N rf channels (one pulse per rotor period of flip-angle θ_1 and amplitude $\omega_{rf,H}^{pul} / (2\pi) = \omega_{rf,N}^{pul} / (2\pi) = 60$ kHz as illustrated for the ¹H→¹⁵N element in Fig. S1). The mixing time was $N=6$ rotor periods (N_1 in Fig. S1), corresponding to 200 μ s. The ¹⁵N→¹³C coherence transfers in Fig. 1e were recorded using a carefully optimized adiabatic variant³ of the DCP experiment⁴ (a tangential shape with $\beta=-500$, $\Delta=2300$ was applied on the ¹⁵N channel; similar shapes were tried for ¹³C channel also but without improving the efficiency) with average rf field strengths of 35 and 65 kHz on the ¹⁵N and ¹³C rf channels during the 3 ms mixing time. For a volume restricted sample (sample extending over the central 2 mm in the axial dimension), the adiabatic DCP experiment provided 64% transfer relative to a corresponding direct-transfer ¹H-¹³C CP/MAS experiment, a number which is reduced to 40% for a full rotor (sample extending over 8 mm in the axial dimension; this dimension was used for all experiments presented). The *RESPIRATION*CP experiment for the ¹⁵N-¹³C transfer used phase-alternated CW irradiation on the ¹⁵N rf channel with amplitude of 30 kHz, while the *RESPIRATION* pulses on the ¹⁵N and ¹³C rf channels used 58 kHz (0.9 μ s duration; i.e., $\theta_2 \approx 19^\circ$ using the notation in Fig. S1). The mixing time was $N=60$ rotor periods (N_2 in Fig. S1), corresponding to 2 ms.

The experiments in Fig. 2g-j used the following parameters. The rf field strengths for the different sequences were varied in a range of [-10,10] kHz relative to the optimum values. For ¹H→¹⁵N transfers, the rf field strengths on the ¹H channel (Fig. 2g) were varied around 70 kHz in case of ramped CP (red) and around 60 kHz for the *RESPIRATION*CP (blue). On the ¹⁵N channel (Fig. 2h) the center is 40 kHz for the ramped CP (Red) and 60 kHz for *RESPIRATION*CP (blue). In Figs. 2i and 2j respectively, the rf field strengths on ¹⁵N and ¹³C were varied during the ¹⁵N→¹³C transfer centered around 35 and 30 kHz on ¹⁵N for the adiabatic DCP and *RESPIRATION*CP, respectively, and around 65 and 58 kHz on the ¹³C channel. The remaining experimental parameters were kept same as in Fig. 1.

In Fig. 3, the resonance-offset dependencies are shown by both simulations and experimental results demonstrating the performances of the various pulse sequences over a range of 20 kHz. The relevant protein/peptide chemical shift ranges in kHz for 400 and 800 MHz spectrometer conditions are shown by the bar and dashed bar respectively. At 800 MHz these ranges (in kHz) are [-2, 2], [-2.5, 2.5], [-1.4, 1.4] and [-1.65, 1.65], respectively, for the ¹H, ¹³C α , ¹³C' and ¹⁵N.

The two 2D experiments in Fig. 4 were recorded with the same optimized parameters as in Fig. 1 using 64 increments in the indirect dimension and with 772 scans per increment.

2. Numerical simulations

All numerical simulations were conducted using the open-source SIMPSON simulation program⁵⁻⁷ using typical amide ¹H, ¹³C α , and amide ¹⁵N chemical shielding tensors and heteronuclear dipolar and J couplings as given in the SIMMOL paper.⁸ The simulations used 20 to 144 *REPULSION* α,β crystallite angles⁹ and 5-18 γ -angles distributed using γ -COMPPUTE.¹⁰ All simulations presented correspond to 9.4 T (400 MHz resonance frequency for ¹H) static field and $\omega_r/2\pi=30$ kHz sample spinning.

The *RESPIRATION*CP simulations in Fig. 1c use phase-alternated CW irradiation with amplitude $\omega_{\text{rf}}=2\omega_r$ at the ^1H channel for $^1\text{H}\rightarrow^{15}\text{N}$ step and at the ^{13}C channel for the $^{15}\text{N}\rightarrow^{13}\text{C}$ step, 2 μs interleaving rf pulses of amplitude 120 kHz (one pulse of flip-angle $\theta \approx 90^\circ$ on each channel per rotor period; virtually identical results are obtained using substantially lower rf amplitudes on these pulses, e.g., 75 kHz ($\theta \approx 54^\circ$) as used in the Fig. 3 simulations). The CP and DCP simulations in Fig. 1c uses constant amplitude rf irradiation with amplitude $\omega_{\text{rf}}=2.5\omega_r$ and $\omega_{\text{rf}}=1.5\omega_r$ on ^1H and ^{15}N , respectively, for the $^1\text{H}\rightarrow^{15}\text{N}$ transfer and $\omega_{\text{rf}}=1.5\omega_r$ and $\omega_{\text{rf}}=2.5\omega_r$ on ^{15}N and ^{13}C , respectively, for the $^{15}\text{N}\rightarrow^{13}\text{C}$ transfer.

The *RESPIRATION*CP simulations in Figs. 2a-2d use phase-alternated CW irradiation on the ^1H channel for the $^1\text{H}\rightarrow^{15}\text{N}$ transfer ($N=7$ rotor period mixing) and on the ^{13}C channel for the $^{15}\text{N}\rightarrow^{13}\text{C}$ transfer ($N=68$ rotor period mixing). The *RESPIRATION* pulses (one pulse on each channel per rotor pulse) were of duration 2 μs implying that the vertical axes in Figs. 2a and 2b correspond to flip angles of $\theta = 0^\circ$ to $\theta = 180^\circ$). The DCP simulations in Figs. 2e and 2f use mixing times corresponding to 5 and 44 rotor periods, respectively.

The *RESPIRATION*CP simulation in Fig. 3a uses CW irradiation ($\omega_{\text{rf}}=2\omega_r$) on the ^1H channel ($N=6$ rotor period mixing) and 75 kHz rf field strength for the 2 μs rf pulses (i.e., $\theta \approx 54^\circ$; we note that the broadbandedness in the ^{15}N dimension increases with increasing power on these pulses). For Fig. 3d the CW irradiation ($\omega_{\text{rf}}=2\omega_r$) is on the ^{13}C rf channel ($N=68$ rotor period mixing), while in Fig. 3f the CW irradiation is on the ^{15}N channel – in both cases 2 μs rf pulses of 75 kHz amplitude is used (i.e., $\theta \approx 54^\circ$).

Acknowledgements

We acknowledge support from the Danish National Research Foundation and the FP7 BIONMR project.

References:

- (1) Wei, D.; Akbey, Ü.; Paaske, B.; Oschkinat, H.; Reif, B.; Bjerring, M.; Nielsen, N. C. Optimal 2H Rf Pulses and 2H- ^{13}C Cross-Polarization Methods for Solid-State 2H MAS NMR of Perdeuterated Proteins. *J. Phys. Chem. Lett.* **2011**, *2*, 1289-1294.
- (2) Metz, G.; Wu, X. L.; Smith, S. O. Ramped-Amplitude Cross-Polarization in Magic-Angle-Spinning Nmr. *J. Magn. Reson. Ser. A* **1994**, *110*, 219-227.
- (3) Hediger, S.; Meier, B. H.; Kurur, N. D.; Bodenhausen, G.; Ernst, R. R. Nmr Cross-Polarization by Adiabatic Passage through the Hartmann-Hahn Condition (Aphh). *Chem. Phys. Lett.* **1994**, *223*, 283-288.
- (4) Schaefer, J.; McKay, R. A.; Stejskal, E. O. Double-Cross-Polarization Nmr of Solids. *J. Magn. Reson.* **1979**, *34*, 443-447.
- (5) Vosegaard, T.; Malmendal, A.; Nielsen, N. C. The flexibility of SIMPSON and SIMMOL for numerical simulations in solid- and liquid-state NMR spectroscopy. *Monatshefte Für Chemie* **2002**, *133*, 1555-1574.
- (6) Bak, M.; Rasmussen, J. T.; Nielsen, N. C. SIMPSON: A general simulation program for solid-state NMR spectroscopy. *J. Magn. Reson.* **2000**, *147*, 296-330.
- (7) Tosner, Z.; Vosegaard, T.; Kehlet, C.; Khaneja, N.; Glaser, S. J.; Nielsen, N. C. Optimal control in NMR spectroscopy: Numerical implementation in SIMPSON. *J. Magn. Reson.* **2009**, *197*, 120-134.

- (8) Bak, M.; Schultz, R.; Vosegaard, T.; Nielsen, N. C. Specification and visualization of anisotropic interaction tensors in polypeptides and numerical simulations in biological solid-state NMR. *J. Magn. Reson.* **2002**, *154*, 28-45.
- (9) Bak, M.; Nielsen, N. C. REPULSION, a novel approach to efficient powder averaging in solid-state NMR. *J. Magn. Reson.* **1997**, *125*, 132-139.
- (10) Hohwy, M.; Bildsøe, H.; Jakobsen, H. J.; Nielsen, N. C. Efficient spectral simulations in NMR of rotating solids. The gamma-COMPUTE algorithm. *J. Magn. Reson.* **1999**, *136*, 6-14.